Available at www.sciencedirect.com

ScienceDirect

journal homepage: www.elsevier.com/locate/issn/15375110

Research Paper

Moisture content and residence time distributions in mixed-flow grain dryers

J. Mellmann [a,*], K.L. Iroba [a,1], T. Metzger [b], E. Tsotsas [b], C. Mészáros [c], I. Farkas [c]

[a] Department of Post Harvest Technology, Leibniz Institute for Agricultural Engineering Potsdam-Bornim (ATB), Max-Eyth-Allee 100, Potsdam D-14469, Germany

[b] Thermal Process Engineering, Otto-von-Guericke-University Magdeburg, Universitätsplatz 5, Magdeburg, D-39106, Germany

[c] Department of Physics and Process Control, Szent István University, 2103 Gödöllö, Hungary

ARTICLE INFO

Article history:
Received 21 January 2011
Received in revised form
19 April 2011
Accepted 21 April 2011
Published online 31 May 2011

Unfavourable designs of mixed-flow grain dryers can cause inappropriate residence time distributions, locally different drying conditions and, hence, inhomogeneous drying. To study the effect of design elements and different air duct arrangements, residence time experiments, grain drying experiments and discrete element simulations were conducted both at pilot and industrial scale. These investigations revealed that present dryer designs give broad distributions of residence time, moisture content, and grain temperature. This is a consequence of different drying histories for individual grains. This variation is mainly influenced by the air duct arrangement applied but is affected by other structural and operating parameters as well. Uneven drying is one of the main reasons for elevated energy demands which are still comparatively high in mixed-flow dryers. A future goal will be to develop improved designs of mixed-flow dryers.

1. Introduction

Mixed-flow dryers (MFDs) are widely used in agriculture to preserve large mass flows of grain (Brooker, Bakker-Arkema, and Hall, 1992; Mühlbauer, 2009; Nellist and Bruce, 1995) but also used in industry. Although this technology has been established for convective grain drying, there is still a need to optimise the process and the drying apparatus. Badly designed elements can cause broad residence time distributions (RTDs), locally different drying conditions and, hence, inhomogeneous drying. As a result, in practise a considerable part of the grain is over-dried. This unnecessary dehydration causes high specific energy consumption, increases costs and reduces quality. It is, therefore, of paramount importance to understand the physical phenomena that control the flow and drying of grains in such equipment to guarantee product quality and minimise the waste of energy, thereby optimising the drying process.

The majority of research papers published on mixed-flow drying have focused on how to increase dryer performance and to save product quality by improving the dryer control. Bruce (1984) applied a multiple-bed computer simulation to model the dryer as a series of concurrent and counter-current elements. The model was successfully employed to predict the general behaviour of the dryer and the influence of operating variables on dryer performance. In a dynamic form this was

* Corresponding author. Tel.: +49 331 5699 321; fax: +49 331 5699849.
E-mail addresses: jmellmann@atb-potsdam.de (J. Mellmann), thomas.metzger@ovgu.de (T. Metzger), Farkas.Istvan@gek.szie.hu (I. Farkas).
[1] Present address: Department of Chemical and Biological Engineering, University of Saskatchewan, 57 Campus Drive, Saskatoon, SK, Canada S7 N 5A9.

1537-5110/$ – see front matter
doi:10.1016/j.biosystemseng.2011.04.010

Nomenclature

n	Number of time intervals, see Eq. (1)
N_{TP}	Number of tracer particles discharged
t	Time, s
Δt	Time interval, s
T_m	Mean residence time, s
x, y	Cartesian coordinates, m

Subscripts

m	mean
TP	tracer particle

Abbreviations

CHP	combined heat and power plant
d.b.	dry basis
DEM	Discrete Element Method
m.c.	moisture content
MFD	mixed-flow dryer
RTD	residence time distribution
w.b.	wet basis

used to develop an automatic dryer controller by McFarlane and Bruce (1991). Different control strategies for mixed-flow dryers have been developed including model-based control, for example by Courtois, Abud Archila, Bonazzi, Meot, and Trystram (2001), Liu, Zhang, Tang, and Lu (2003), and Liu, Chen, Wu, and Zhang (2006).

Relatively little research has been published on individual processes such as air flow and grain flow in MFD. Cenkowski, Miketinac, and Kelm (1990) simulated and measured air flow patterns and isobars in a full-scale section of a conventional MFD. The differential equation system derived was solved using the finite element method. Although a semi-empirical relationship for a static bed was implemented, the authors achieved an acceptable agreement with the measurements. The authors reported that cross-flow elements occupy about 30% of the dryer volume, hence, they should be considered. Chaabouni, Flick, and Techasena (1992) investigated the particle flow in MFDs based on the residence time analysis using coloured tracer particles. The authors applied a two-dimensional flow model which was a combination of the continuity equation with a probabilistic approach of transversal particle displacement. It was found that this model gave a good prediction of the deformation of the tracer particle layer and the RTD based on parameter estimation. However, the numerically calculated particle trajectories differed from the measurements.

To simulate heat and mass transfer in industrial mixed-flow dryers for maize, Sun, Arnaud, and Fohr (1992) developed a two-dimensional model in a static bed of grain in a small section of the dryer between one inlet and one outlet air duct. The model combines air flow, heat and moisture transfer between air and grain considering particle trajectories. The differential equation system was solved using the finite element method. The authors presented numerical results showing flow lines, isobars, as well as temperature and moisture distributions in the domain. The results showed there is a high density of streamlines under the edges of the air ducts and, hence, high air velocities. The authors concluded that over-drying can be expected around the edges of the hot inlet air ducts. However, a comparison between measured and predicted results was not given. Giner, Bruce, and Mortimore (1998) developed a two-dimensional simulation model to predict moisture and temperature distributions as well as viability loss of the grain bed. The dryer was subdivided into blocks describing a vertical slice through the dryer. Each block consisted of one-dimensional elements of concurrent, counter, and cross-flow beds. The way the blocks were formulated allowed the model to differentiate between grains flowing down the dryer near the inlet or exit air ducts. Giner and Bruce (1998) tested this model in a laboratory-scale mixed-flow dryer. In this case, a set of eleven drying experiments were evaluated. For given inlet and outlet grain moistures, the 2D model predicted the trends of the mean moisture content and grain viability over the dryer height relatively well. However, the moisture differences were underestimated between zones close to inlet and exit ducts. Exit air temperatures were generally overestimated.

More recently, the number of papers related to basic research on MFD has increased. Cao, Yang, and Liu (2007) used a simulation model in order to investigate the effect of structural and operating parameters on the performance and energy consumption of a mixed-flow grain dryer. The simulations conducted were based on a two-dimensional dryer model which has been developed in a previous work (Liu, 1993). The authors put special emphasis into studying the effect of structural parameters such as size and shape of air ducts, the spacing between air ducts, the number of rows of air ducts, and column height. They showed that small air ducts are better than large air ducts. Mellmann, Richter, and Maltry (2007) derived a model for the coupled heat and mass transfer in MFDs which was tested in pilot scale experiments for hot-air drying farm-fresh wheat. The work was primarily aimed at developing a concept for a model-based dryer control. For the grain mass flow, however, a simple plug-flow approach was used. Kocsis et al. (2008) reported on experimental findings of the influence of air ducts and side walls on grain flow. Particle velocity and mass flow distributions were measured at an MFD test station equipped with a transparent acrylic glass front wall. It was shown that the particle flow through the centre of the dryer is faster than at the side walls. To simulate the particle movement in mixed-flow dryers Iroba, Weigler, Mellmann, Metzger, and Tsotsas (in press), 2011 developed a two-dimensional model based on the discrete element method (DEM). To validate the model and to detect particle flow inhomogeneities due to design problems, the authors employed the residence time analysis using coloured tracer particles in the MFD. It was shown that two flow regions exist in MFDs, a near-wall region with low particle velocity, and a central region with high particle velocity. Wall friction has a large effect on bulk particle movement. Wall friction dominates in the near-wall region whereas particle–particle forces are dominant in the central region. Thus, grains in MFDs have different vertical velocities, resulting in different residence times. A comparison between simulated and experimental results revealed that the DEM can adequately predict the main features of particle flow. Based on the analysis of particle

trajectories, Iroba, Mellmann, Weigler, Metzger, and Tsotsas (2011), demonstrated that half the air ducts positioned at the side walls of the dryer created obstructions to the free flow of grains. As could be seen both in experiment and simulation, the corners under the half air ducts provided dead zones for particle flow where the tracer particles resided extremely long times. Thus, grains flowing down the dryer in the near-wall region are in danger of being over-dried. Mellmann and Teodorov (2011) developed fundamental equations on solids transport in mixed-flow dryers equipped with discharge gates. Based on experiments on the discharge characteristic of an MFD test dryer, the authors derived an equation for the solids mass flow rate for the practically relevant interrupted flow regime.

Despite the previous investigations of the individual processes of air and grain flow and some continuous models, there are still a number of problems associated with mixed-flow dryers that result in the non-uniform moisture distribution of grains at the outlet. This study aims to investigate the effects of design elements and different air duct arrangements on drying in MFDs. Because of their interrelation in the drying process, both residence time and moisture content distributions were investigated. To evaluate the evenness of drying, grain moisture and temperature distributions were measured in drying experiments that were conducted at both pilot plant and industrial scales.

2. Materials and methods

2.1. *Experiments on grain moisture, temperature, and residence time distributions*

To study the grain residence time, moisture content, and temperature distributions, particle flow and drying experiments were conducted using pilot plant and industrial scale dryers. Industrial mixed-flow dryers are mostly operated under quasi-continuous conditions in a record-by-record (interrupted) mode. During the main part of the drying time, the grain bed is at rest while it is vertically transported only intermittently when the discharge device is opened. In this manner, the grains move stepwise from the top to the bottom of the dryer under gravity. For the grain drying experiments, the test dryer was operated in the practical interrupted flow regime.

With respect to the particle flow in MFD, two modes of operation are possible in principle: interrupted flow and continuous flow (Iroba, et al. 2011, in press). The continuous flow mode can be regarded as a special case of the interrupted flow mode where the discharge time is infinite, e. g. the discharge device is steadily opened and the grain flows out unrestricted and continuously. It is comparable with the outflow of solids from a silo where the maximum discharge rate is achieved (Mellmann & Teodorov, 2011). Although the continuous flow regime is not of practical relevance, it is of high theoretical relevance with regard to particle flow studies. In the continuous flow mode, the particle flow behaviour can be investigated more easily than in interrupted flow mode. This is because the flow just depends on the apparatus geometry and the physical properties of the bed material.

Hence, the continuous flow mode was adopted for the DEM simulation of particle flow. As a result computational time and resources could be saved as compared to the (non-continuous) interrupted flow simulation. In contrast to the DEM simulation, continuous flow cannot be applied in the residence time experiment. This is due to the size of the test dryer and the bed material handling. It would not be possible to properly collect the large masses of grains and tracer particles discharged and to refill the dryer under conditions of continuous flow. Therefore, interrupted flow was adopted. To evaluate the data only the discharge times were assessed assuming that continuous flow occurred during these periods(see Iroba et al., 2011, in press).

Fig. 1 illustrates the test dryer of the Leibniz Institute for Agricultural Engineering, Potsdam, Germany. The test station consists of two parallel vertically arranged dryer shafts: one is used for grain flow studies, the other for drying experiments (Mellmann et al., 2007). The dryer is fed by an elevator conveying the grain to the filling section at the top. It is connected with an air conditioning system and a computer-based measuring and control device. The dryer shaft, of about 2 m height (0.6 m times 0.4 m in cross-section), consists of in total 26 inlet and outlet air ducts which are horizontally aligned across the dryer depth.

The test dryer is equipped with a pneumatically operated discharge gate to release batch-wise the grain and to control the mass flow rate providing an even grain flow over the cross-section. The air duct arrangement can be changed using lock plates at both sides of the dryer shaft. Thus, individual inlet or exit air ducts can be closed or opened, respectively. To measure the grain moisture content and temperature distributions at the dryer discharge, a set of 40 sampling boxes (80 mm $\times$ 80 mm each) were employed at the discharge end, see Fig. 2. With the pilot scale experiments wheat was used as the bed material.

2.2. *Discrete element model for residence time simulation*

In the simulation, a mixed-flow dryer equipped with a discharge gate was considered. The DEM (Itasca, 2004) computed the particle flow numerically using an explicit time integration scheme with suitable boundary and initial conditions. The inter-particle force models were also applied to the interaction between a particle and a wall with the corresponding wall properties used. However, the wall was assumed to be so rigid that no displacement and movement resulted from this interaction.

The dimensions of the experimental and simulated dryers are shown in Fig. 3 (a & b). The actual shape of wheat is nearly ellipsoidal. This particle shape was used by Markauskas, Kačianauskas, Džiugys, and Navakas (2010) to simulate the piling problem. The authors adopted a multi-sphere model to compose ellipsoidal particles. However, non-spherical particles require more advanced algorithms and are more difficult to model (Luding, 2008). Hence, spherical particles were used for the simulation. In this work, the linear-elastic contact model was applied because it is the easiest, simplest and fastest contact model. The particle size used was large enough that van der Waals forces played no role. Thus, normal stiffness and shear stiffness were set equal to each other. The mean equivalent spherical particle diameter and the bulk density of wheat were obtained from our own measurements, and the other properties were taken from literature (Kunibert, 1983; Mohsenin, 1970; Sokhansanj & Lang, 1996).

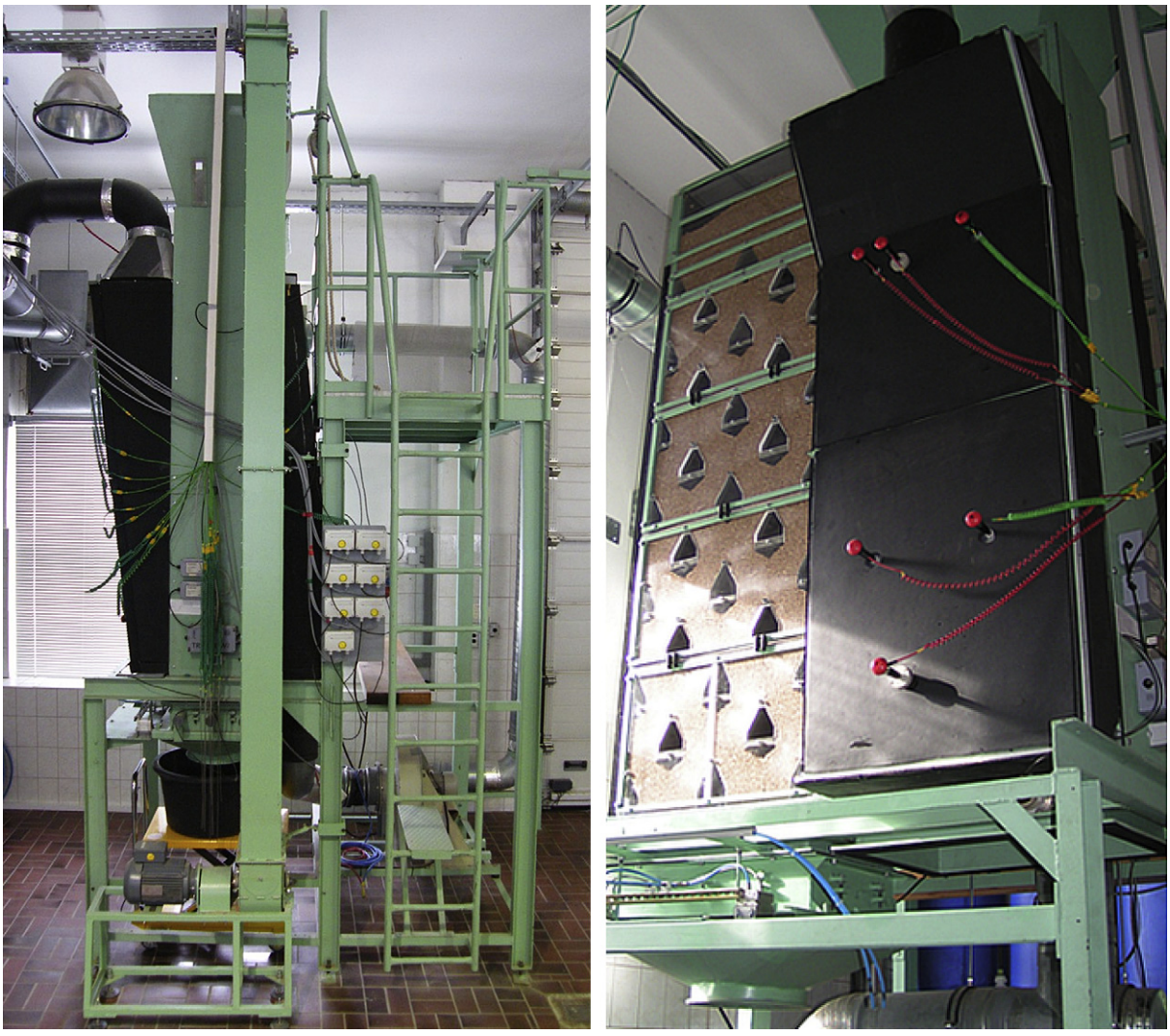

Fig. 1 – Pilot scale MFD test station, ATB, Potsdam, Germany.

Fig. 2 – Measuring boxes at the dryer discharge.

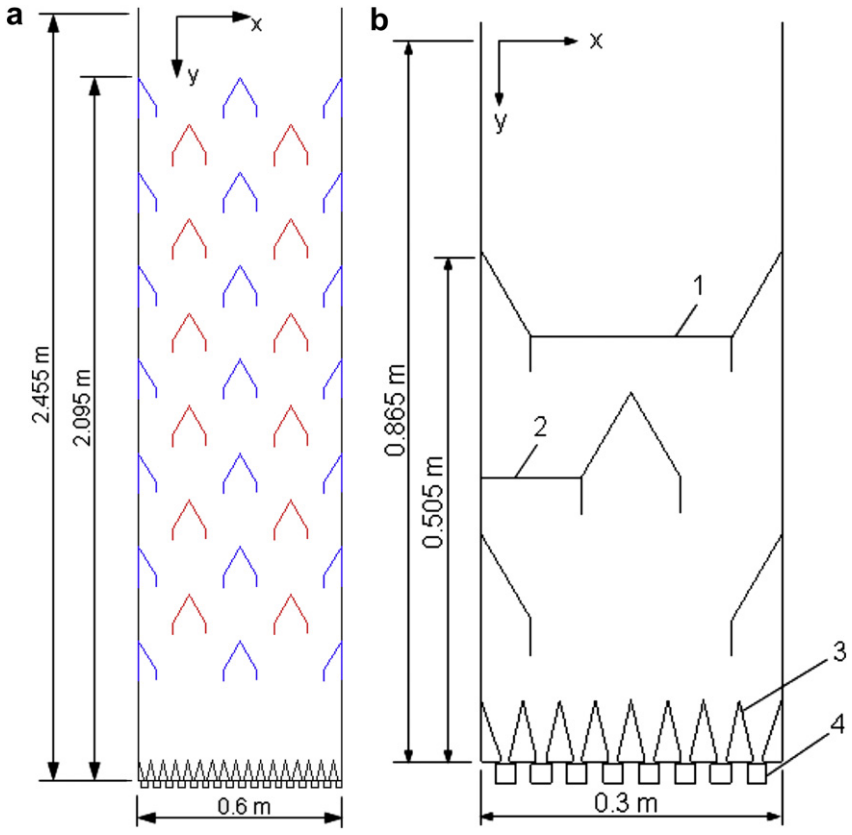

Fig. 3 – Schematic of the a) MFD test station. b) simulated dryer. 1, 2 – layers where particle velocities were monitored. 3, 4 – Fixed and moving parts of the bottom discharge device, respectively.

The assumptions involved in the simulation of the particle flow can be summarised as follows:

1. The geometry of the dryer is constant over the depth, hence, two-dimensional model was adopted.
2. The dryer geometry simulated comprises ½ of the width of the test dryer.
3. The length of flow in the simulation is about ¼ of the length of flow in the experiment, see Fig. 3 a & b.
4. The single wheat grain is modelled as a spherically shaped particle.
5. Continuous flow mode is considered.
6. It was assumed that there is no air flow.

Only a part of the real dryer geometry was modelled in order to save on computational time. The computational domain where particle velocity profiles were monitored during the simulation (Iroba et al., 2011,) was placed above the discharge device, see Fig. 3b. The cross-sections of the air ducts and the bottom discharge device were consistent with the real dimensions of the test dryer. To simplify the model and to save computational time and resources, single grains were modelled as spherically shaped particles. For the same reason, the continuous flow mode was considered in the simulation of particle motion. The definitions of the two flow regimes and the advantages of the continuous flow mode are illustrated in Section 2.1. In the DEM model, the influence of air flow was neglected. For more details on the DEM simulation, see Iroba et al. (2011).

3. Results and discussion

3.1. *Residence time distribution (RTD)*

The differences in particle movement between the near-wall and central regions was investigated in detail by determining the RTD in the dryer with the help of tracer particles, which were introduced at the top of the equipment (Iroba et al., 2011, in press). The residence time of the particles as they flow down the dryer is a function of their positions over the cross-section of the dryer.

3.1.1. *Simulation*

In the RTD simulation 400 mono-dispersed yellow coloured grains were used as tracer particles. The geometry of the dryer used and the layer of yellow tracer particles at the beginning of the RTD simulation are shown in Figs. 3b and 4a, respectively.

The discharge time, the real time it took the tracer particles to vertically move from their starting position (see Fig. 4a) through the dryer geometry till discharged point was 7.36 s. The histories of the y-positions with time of the yellow tracer particles were monitored. Fig. 4b depicts the tracer particles in the course of the simulation. As this figure shows, the particle flow through

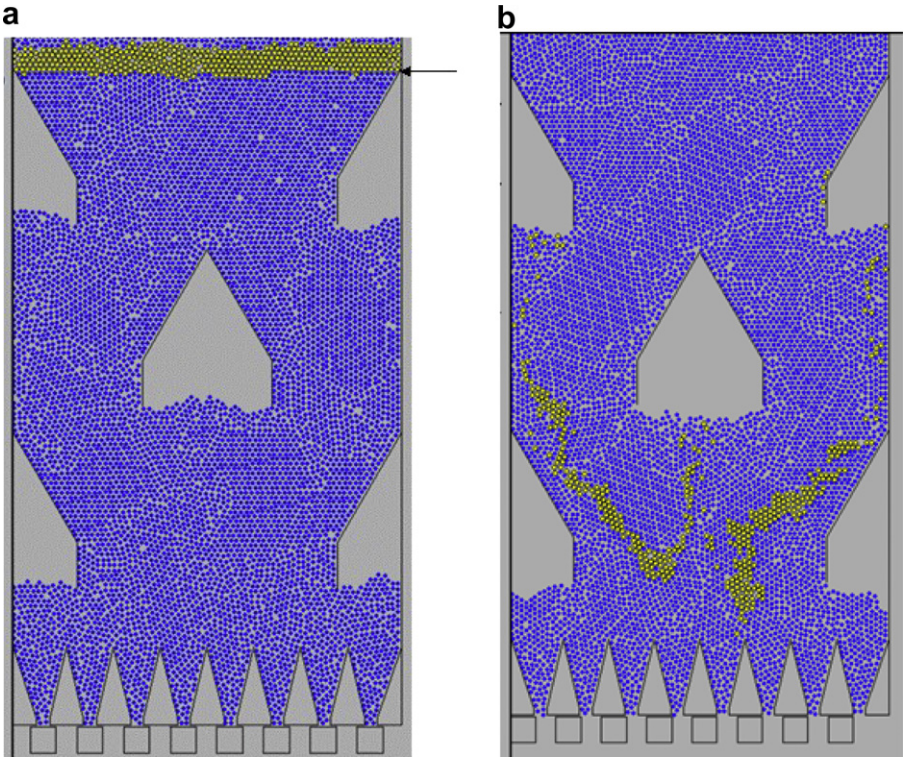

Fig. 4 – a) Layer of yellow coloured tracer particles at the beginning of the RTD simulation, starting position (arrow) b) Deformation of the tracer particles stripe in the course of the simulation.

the centre of the dryer was faster than at the side walls where friction restricts the free motion thereby retarding the flow.

The number of yellow particles discharged, and the time taken for each of them to travel from the top lattice position to the bottom of the dryer, were monitored and computed, respectively. This time represents the residence time of the particles. The graphical representation of the calculated RTD is given in Fig. 6. For direct comparison of the RTDs obtained from simulation and experiment their coordinates were transformed to dimensionless variables. The break-through time, i.e. the time taken for the first tracer particle to leave the dryer was 2.25 s. At the end of the simulation, 99% (i.e. 396) of the yellow particles used for residence time calculation were recovered from the dryer while 1% (which represents four particles) was left in the dryer.

$$T_m = \frac{\sum_{i=1}^{n} N_{TP,i} \cdot t_i \cdot \Delta t}{\sum_{i=1}^{n} N_{TP,i} \cdot \Delta t} \quad (1)$$

The mean residence time was calculated with a time class interval Δt of 0.10 s using Eq. (1), resulting in a value of

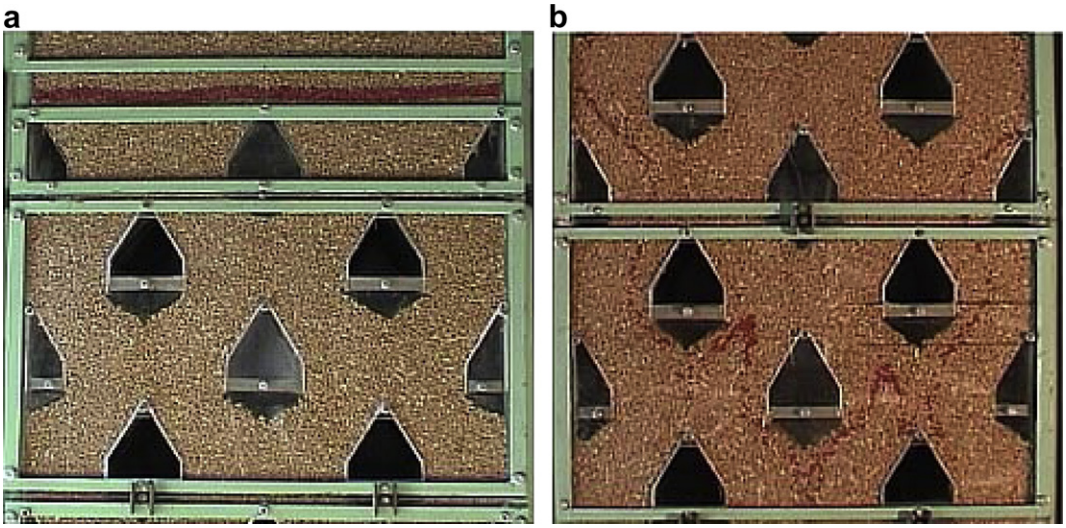

Fig. 5 – a) Layer of red coloured tracer particles at its starting position b) Flow pattern of the tracer particles.

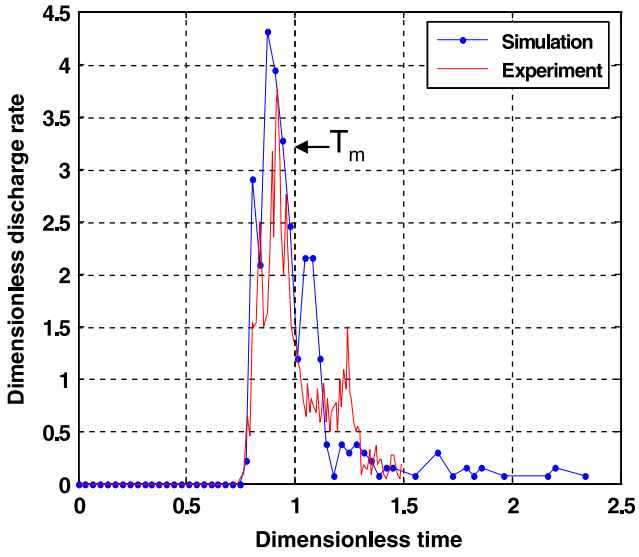

Fig. 6 – Comparison between simulated and experimental RTD: T_m = mean residence time.

$T_m = 2.97$ s. Iroba et al. (2011), also studied the trajectories of the tracer particles to further study the flow behaviour of discrete particles and to analyse flow obstructions.

3.1.2. *Experiment*

At first, the test dryer was filled with wheat by means of the elevator up to the first horizontal row of exit air ducts from the top, see Fig. 3a. This is approximately 0.36 m from the top of the dryer. To measure the residence time, coloured wheat grains were used as tracer particles. The bed surface was horizontally levelled and smoothed. To approximate a Dirac pulse, a horizontal layer of 2400 red coloured tracer particles was carefully arranged at the top of the bed close to the transparent acrylic glass front wall. This layer covered the total width of the dryer, 0.6 m, with a height of 0.02 m and a thickness (depth) of 0.01 m. The tracer particle layer was visible at the front of the dryer, see Fig. 5a. The length of flow of the tracer particles in the experiment was 2.095 m (Fig. 3a). The RTD was measured by counting the coloured particles in the discharged grain samples. The experiment was recorded using a digital video camera. Fig. 5b shows the deformation of the layer in the course of the experiment. The discharged mass of grains per loop (opening and closing cycle of the discharge device) was always weighed using a balance and the numbers of tracer particles in each discharge sample were carefully counted by spreading each sample on a wide flat tray.

The discharge continued in this sequence of single loops until about 73% of the tracer particles had left the dryer. Throughout the experiment the dryer was continuously refilled. In this manner the RTD has been measured as shown in Fig. 6. The break-through time measured was 24.3 s. Using Eq. (1) with a time class interval Δt of 0.30 s, the mean residence time T_m was determined as 32.6 s.

It was calculated only for the 73% discharged coloured tracer particles (1756) that were collected from the discharge samples. The remaining 27% (644) were trapped at the side walls of the dryer between the half air ducts (corners). It should be noted that after collecting 73% of tracer particles, the dryer was emptied in a stepwise discharge manner (i.e. open and close order); coloured grains were still found even in the last portion of grains that was discharged. This implies that those tracer particles at the corner of the dryer could reside in the dryer shaft throughout the grain flow experiment. As can be expected, these grains would be excessively over-dried in the real drying process.

For the purpose of direct comparison of the RTDs obtained from simulation and experiment, their coordinates were transformed into dimensionless discharge rate and time. As is clear from the graphs in Fig. 6, the measured and calculated dimensionless RTDs are in close agreement. The flow profiles of particles in the simulation and in the experiment are consistently similar. The peaks represent the tracer particles that flow through the centre of the dryer with higher particle velocities and lower friction effect. The long tails revealed the influence on the grain flow of wall friction and the half air ducts positioned directly at the side walls. These particles travel with lower vertical velocities due to higher frictional effects. As a result, grains have different residence times in the dryer, see also Cao et al. (2007). The consequence of this is that there will be uneven moisture distribution within the bulk of grains during the drying process, with the risk of product quality loss during subsequent storage. Grains with higher velocities may be under-dried and those with lower velocities may be over-dried depending on the required drying time. Over-drying is costly in three ways:

- There is excessive shrink, and less weight is sent to the market;
- There is extra drying cost (energy) for removing too much moisture;
- Thermal damage may occur.

3.2. *Grain moisture content and temperature distributions*

Besides the particle flow, the drying process in total is affected by design elements such as air duct arrangement, and side walls (half air ducts). This will be demonstrated in this section where grain moisture content and temperature measurements are evaluated. The data were obtained from drying experiments both at semi-technical and industrial scale under steady-state conditions. First results have already been presented by Kocsis, Farkas, Mészáros, Teodorov, and Mellmann (2009) and Mellmann, Iroba, Möller, Metzger, and Tsotsas (2010).

In a mixed-flow dryer, air and grain are guided through the dryer shaft in co-current, counter-current and cross-flow modes at the same time (Pabis, Jayas, & Cenkowski, 1998). To distribute the drying air over the grain bulk material filled in the dryer shaft, inlet and outlet air ducts are arranged and allocated in a certain manner. Mostly, they are horizontally arranged across the dryer depth.

In Fig. 7 the two major air duct arrangements in MFD are shown over the vertical cross-section with (+) characterising an inlet and (−) exhaust air ducts, respectively. Typically, the air ducts are arranged in this shifted and symmetric form. The

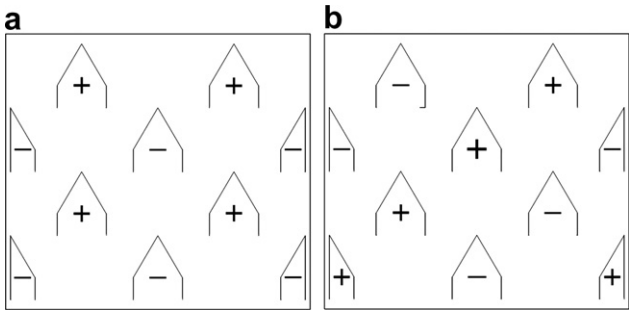

Fig. 7 – Air duct arrangements in MFD: a) horizontal (classical); b) diagonal, Schmidt-Seeger GmbH, Beilngries, Germany.

air duct arrangements illustrated exactly correspond to those which have been installed in the test dryer shown from the inlet air side view. It should be mentioned that the air duct rows containing the half air ducts are mainly employed for inlet air supplyin industrial dryers. This is to avoid blocking of the half air ducts due to high humidity and dust in the exit air. The classical type is the horizontal arrangement (Fig. 7a) where rows of inlet and exhaust air ducts alternate from the top to the bottom of the dryer. This mode of air duct arrangement is widely used by many dryer manufacturers. More recently, a new diagonal air duct arrangement has been proposed (Schmidt-Seeger, Germany), see Fig. 7b. In this case, rows of inlet and outlet air ducts alternate in diagonal direction. Both types of air duct arrangement have advantages and disadvantages. They will be compared to each other based on pilot scale drying experiments.

3.2.1. *Pilot scale experiments*

To compare the classical horizontal with the diagonal air duct arrangements, various drying experiments were been conducted. The settings of the experiments selected are listed in Table 1. After steady-state was reached, the measuring boxes were placed under the discharge end using a hand lift (Fig. 2). The total grain mass of one dryer discharge loop was then collected in the boxes. Immediately after the discharge, the grain temperature distribution was determined using a thermal imaging camera (VARIOSCAN 3021-ST, Jenoptik AG, Jena, Germany). Thereafter, the mass flow distribution was measured using a balance. The samples were then taken to determine the moisture content distribution over the cross-section based on drying chamber measurements according to the ISO 712 standard.

The results of two selected experiments at the test dryer are shown in Fig. 8 where the moisture content (m. c.) is shown over the dryer width. Each measuring value represents an average of five measuring points over the dryer depth. As the graphs clearly illustrate, the m. c. strongly fluctuated over the dryer width.

For the horizontal arrangement (experiment 1), the single m. c. values varied from 10.2 to 15.2% w.b. over the whole cross-section. This variation was in the same range as the total difference between inlet and outlet m.c. of 4.0% w.b. (16.8–12.8% w.b., see Table 1) attained in the experiment. The reason for this sinusoidal curve (Fig. 8) was found in the air duct arrangement. Because of the horizontal shifted arrangement, air ducts of the same type (inlet = hot, exhaust = cold) are placed under each other as vertical rows, see Fig. 3a and 7a. Accordingly, single particle trajectories just pass vertical rows of hot inlet or (relatively) cold exhaust air ducts, respectively. Hence, such "streaks" of grain may be over or under-dried. This effect has already been found by Giner and Bruce (1998). As the lower curve in Fig. 8 illustrates, the m.c. minima exactly occurred under the vertical rows of hot inlet air ducts whereas the m.c. maximum in the middle of the dryer was placed under the vertical exhaust air duct row.

These results were confirmed by appropriate grain temperature measurements from the same experiment. Fig. 9 shows thermal imaging camera images taken from the measuring boxes under the dryer discharge. As the comparison for experiment 1 revealed, the positions of the minima of the m.c. distribution in Fig. 8 agree well with those of the maxima of the temperature distribution (Fig. 9a) and vice versa.

As expected, with the diagonal air duct arrangement (Fig. 7b) the moisture content fluctuations were reduced as the upper curve in Fig. 8 illustrates. Both, the amplitude and

Table 1 – Settings of selected pilot and industrial scale drying experiments.

Experiment No.	1	2	3
Dryer	pilot	pilot	industrial
Air duct arrangement	horizontal	diagonal	horizontal
Type of grain	wheat	wheat	barley
Inlet m.c. [% w.b.]	16.8	17.7	14.4
Outlet m.c. [% w.b.]	12.8	14.4	14.0
Grain mass flow rate (dried) [kg h^{-1}]	150	100	25,000
Inlet air temp. [°C]	70	60	40-45
Drying rate [kg [H_2O] h^{-1}]	7.2	4.0	116.8

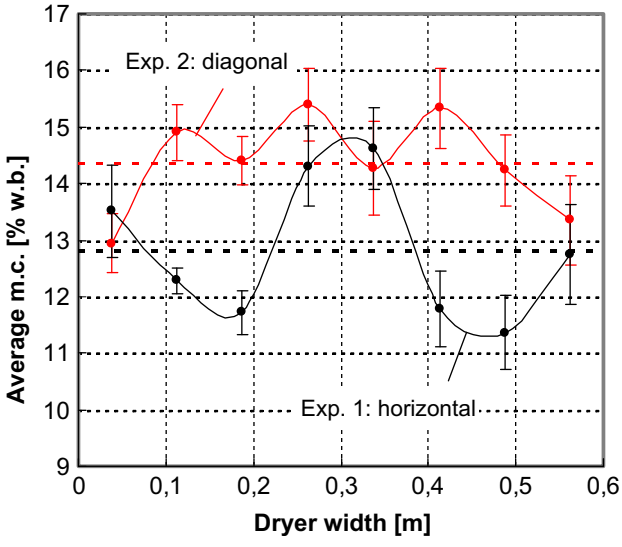

Fig. 8 – Average m. c. as a function of dryer width, measured at pilot scale for horizontal (Exp. No. 1) and diagonal air duct arrangement (Exp. No. 2), see Table 1.

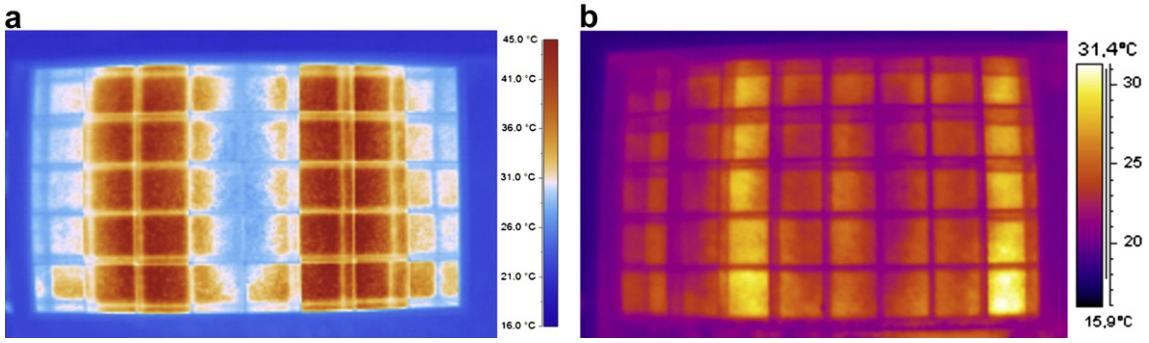

Fig. 9 – Grain temperature distributions measured over the cross-section at dryer discharge: a) horizontal (Exp. No. 1); b) diagonal arrangement (Exp. No. 2), see Table 1.

period of the sinusoidal distribution were nearly halved. However, single m. c. values also varied widely over the cross-section between 12.1 and 15.9% w.b. Again, this variation is in the same range as the total difference between inlet and outlet average m.c. of 3.3% w.b. (17.7–14.4% w.b., see Table 1) attained in the experiment. In the diagonal arrangement, hot inlet air ducts were always among the half air ducts. Thus, the moisture distribution steeply decreased towards the side walls. As already mentioned above (see Fig. 6), this was due to the fact that the particle residence time is highly extended in the near-wall region by the half air ducts fixed at the side walls, where over-drying is more pronounced.

Undoubtedly, the diagonal arrangement gives a more even grain moisture and temperature distribution. However, this advantage is removed by the disadvantage that the air flow distribution in the grain bed is considerably degraded in comparison to the horizontal arrangement. In the diagonal arrangement, dead zones exist in dryer which are not flushed by the drying air. In addition, for the same mass flow rate of the drying air, the air velocity in the grain bed is increased (i.e. almost doubled) due to the air duct allocation. Hence, the drying potential of the inlet air is only partly exploited and dryer performance is reduced. The lower dryer performance of the diagonal arrangement was confirmed by comparing experiments 1 and 2 with respect to the m.c. difference measured between inlet and outlet as well as the drying rate, see Table 1. The average m.c. in experiment 2 was just reduced by 3.3% w.b. Against, in experiment 1 with the horizontal arrangement the total difference between inlet and outlet m.c. was 4.0% w.b. even if the grain mass flow rate was 50% higher. As a result, the drying rate of 7.2 kg [H_2O] h^{-1} attained with the horizontal air duct arrangement in experiment 1 is about 1.8 times higher than the value measured in experiment 2 for the diagonal arrangement as 4.0 kg [H_2O] h^{-1}.

3.2.2. *Industrial scale experiments*

The effect of the air duct arrangement on the grain moisture content distribution has been studied at industrial scale drying experiments as well. The aim of these experiments was to demonstrate the uneven drying observed at pilot scale (Mellmann et al., 2010). For this purpose, the operation of a large scale mixed-flow dryer was accompanied in the harvest season 2009 by moisture content and temperature measurements. Barley was used as the fresh produce (manufacturer: Petkus GmbH, Wutha-Farnroda, Germany; location: Ivenack, Germany). The dryer with a cross-section of 2.3 m by 1.9 m was equipped with a horizontal air duct arrangement according to Fig. 7a. Each horizontal air duct row consisted of eight full air ducts (inlet air: 7 full + 2 half; exhaust air: 8 full air ducts). The main operational parameters are listed in Table 1. The dryer was operated at relatively low air temperatures between 40 and 45 °C. This was due to the low inlet moisture content of 14.4% w.b. of the farm-fresh barley. Hence, to dry this product it was sufficient to use the waste heat from a combined heat and power plant (CHP) at an adjacent biogas plant. The dryer was connected with the CHP via a water circulation and a separate heat exchanger.

The results are illustrated in Fig. 10 where the grain moisture content is shown over the dryer width. In turn, each measuring value represents an average over the dryer depth (i.e. three measuring points). As can be seen from the graph, the grain moisture content strongly oscillates over the dryer width showing seven minima (7 full inlet air ducts) and eight maxima (8 full exhaust air ducts). Again, the minima occur at those

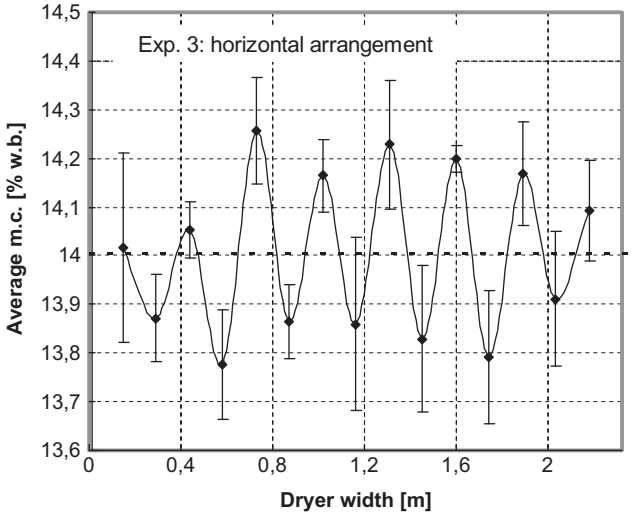

Fig. 10 – Average m. c. as a function of dryer width, measured at an industrial mixed-flow dryer with horizontal air duct arrangement (dryer width 2.3 m).

positions where vertical rows of warm inlet air ducts are located, and vice versa. From the half inlet air ducts no samples were taken, hence, just the seven measuring points (minima) at the inlet air side occurred. This effect of the horizontal air duct arrangement observed in the pilot plant experiment could clearly be approved even if the total difference between inlet and outlet m.c. was just 0.4% w.b. (from 14.4 to 14.0% w.b., see Table 1). This difference is in the same range as the variation of the single measuring values, see Fig. 10.

The unevenness of drying in MFD was confirmed as well by single kernel moisture measurements which have been conducted in a former project at several industrial grain dryers in the harvest season 2004. For this purpose grain samples were taken at a time from the inlet and outlet of the respective dryer during steady-state operation. The type of grain was wheat in all experiments. Firstly, a sample was taken from the farm-fresh grain flow at the inlet. After one mean residence time elapsed, then a sample from the dryer discharge was taken. Each sample amounted to 1–2 kg. To measure the particle moisture distribution of each grain sample, 100 individual grains were selected at random. To avoid dehydration during transportation, the kernels were immediately put into small airproof plastic casings, separately. The moisture distributions of the 100-kernel-samples were measured by non-destructive oven drying in a vacuum chamber. The kernels were placed onto thin alumina plates with numbered cavities for the grains. Each plate captured 25 single grains. The samples were then dried in the vacuum drying chamber for 24 h at 105 °C and the lowest adjustable pressure of 8 kPa. In preparation for the experiments, the vacuum drying method was calibrated against the standard drying method according to ISO 712. Using the calibration function, the measured particle moistures have been converted. The moisture distributions obtained from the 100-kernel-samples could be well approximated by the Gaussian distribution.

The results of the single kernel moisture distributions obtained are shown in Fig. 11 at the example of one selected industrial mixed-flow dryer. This dryer was equipped with the horizontal air duct arrangement (Fig. 7a). The two curves represent the normal moisture distributions at the inlet and outlet of the dryer. As the figure illustrates, the inlet moisture distribution of the farm-fresh wheat (mean m.c. 15.6% w.b.) was relatively narrow and high. As expected, after drying the particle moisture distribution was reduced to lower moisture values. However, the outlet moisture distribution was considerably broadened in comparison to the inlet. This widening of the moisture distribution was caused by the inhomogeneous drying process and reflected in different drying histories of single grains. It has been detected at other industrial MFDs from different dryer manufacturers as well. Under ideal drying conditions, such as thin-layer drying, a narrowing of the particle moisture distribution would occur during the course of drying as has been observed by Liu, Montross, and Bakker-Arkema (1997). This is because kernels of lower moisture content dry more slowly than kernels of average moisture and kernels of higher moisture content dry faster. In real dryers, however, the drying conditions are different resulting in different drying histories for single grains. With mixed-flow dryers, the variation of the drying histories is mainly influenced by the air duct arrangement as well as other structural and operating parameters.

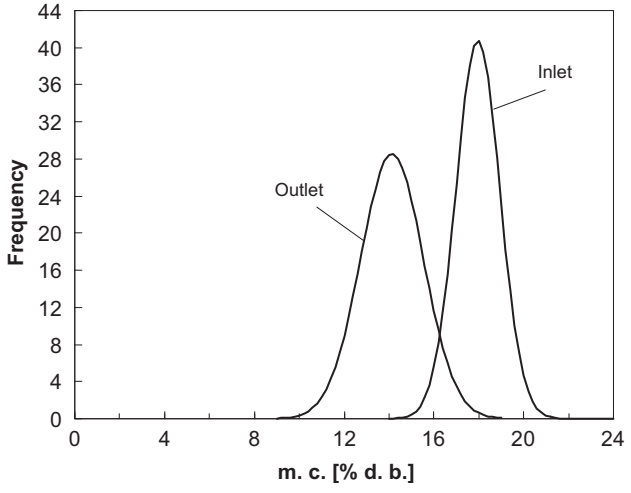

Fig. 11 – Particle moisture distributions measured at the inlet and outlet of an industrial mixed-flow dryer (type: DK 24). Grain species: wheat. Inlet m.c.: 15.6% w.b., outlet m.c.: 12.5% w.b.

4. Conclusions

Moisture content and residence time distributions were investigated in order to study the effect of design elements on the drying process and to better understand the physical phenomena that control the particle flow in MFDs. Concerning the RTD in mixed-flow dryers, comparisons between simulated and experimental results revealed that the DEM can adequately predict the main features of particle flow. The results obtained show that two regions exist in MFDs: a central region with high particle velocity, and the near-wall region with low particle velocity. The half air ducts at the side walls pose a considerable obstruction to the free flow of grains resulting in the long tail of the RTD.

To study the effect of design elements on the uniformity of drying, steady-state drying experiments have been evaluated which were conducted both at pilot and industrial scale. For this purpose, grain moisture content and temperature distributions were measured at the dryer discharge. The effects of the two major air duct arrangements – horizontal and diagonal – were investigated. As these measurements revealed, grain bulk and particle moisture content as well as grain temperature distributions strongly fluctuate over the cross-section and, hence, give inhomogeneous drying. This occurred under steady-state conditions and even with constant inlet moisture content over time (pilot scale experiments). Thus, “streaks” of grain may be over or under-dried resulting in increased energy consumption and loss of product quality. The analysis displayed deficits in the present design of MFDs, namely the arrangement and allocation of the air ducts. According to Maier and Bakker-Arkema (2002) the optimum shape, size and location of the air ducts in the drying bed of a mixed-flow dryer have not been established. Minimising the non-uniformity of drying is a requirement for

this dryer type. A future goal should be to develop new, better designs of mixed-flow dryers.

Acknowledgements

The authors are grateful to the German Federal Ministry for Education and Research for financial support (BMBF/PTJ Project No. 0339992A, TP1.3).

REFERENCES

Brooker, D. B., Bakker-Arkema, F. W., & Hall, C. W. (1992). *Drying and Storage of grains and Oilseeds*. New York: Van Nostrand Reinhold.

Bruce, D. M. (1984). Simulation of multiple-bed concurrent-, counter-, and mixed-flow grain driers. *Journal of Agricultural Engineering Research, 30*, 361–372.

Cao, C. W., Yang, D. Y., & Liu, Q. (2007). Research on modeling and simulation of mixed-flow grain dryer. *Drying Technology, 25*, 681–687.

Cenkowski, S., Miketinac, M., & Kelm, A. (1990). Airflow patterns in a mixed-flow dryer. *Journal of Canadian Agricultural Engineering, 32*, 85–90.

Chaabouni, M., Flick, D., & Techasena, O. (1992). Particles flow in industrial grain driers. Drying '92. In A. S. Mujumdar (Ed.), *Proceedings of the 8th International drying Symposium (IDS'92), Montreal, Canada, August 2-5, 1992* (pp. 1409–1418). Amsterdam: Elsevier Science Publishers B.V.

Courtois, F., Abud Archila, M., Bonazzi, C., Meot, J. M., & Trystram, G. (2001). Modeling and control of a mixed-flow rice dryer with emphasis on breakage quality. *Journal of Food Engineering, 49*, 303–309.

Giner, S. A., Bruce, D. M., & Mortimore, S. (1998). Two-Dimensional simulation model of steady-state mixed-flow grain drying. Part 1: the model. *Journal of Agricultural Engineering Research, 71*, 37–50.

Giner, S. A., & Bruce, D. M. (1998). Two-Dimensional simulation model of steady-state mixed-flow grain drying. Part 2: experimental Validation. *Journal of Agricultural Engineering Research, 71*, 51–66.

Iroba, K.L., Weigler, F., Mellmann, J., Metzger, T., & Tsotsas, E. Residence time distribution in mixed-flow grain dryers. *Drying Technology*, 29, in press.

Iroba, K. L., Mellmann, J., Weigler, F., Metzger, T., & Tsotsas, E. (2011). Particle velocity profiles and residence time distribution in mixed-flow grain dryers. *Granular Matter, 13*, 159–168.

Itasca Consulting Group, Inc.. (2004). *PFC 2D, Version 3.1, Theory and Background Manual*. Minneapolis, USA.

Kocsis, L., Teodorov, T., Mellmann, J., Gottschalk, K., Mészáros, C., & Farkas, I. (2008). Analysis of grain flow experiments in a mixed-flow grain dryer. In *Proceedings of the 17th World Congress of International Federation of automatic control (IFAC)* (pp. 1608–1612). Seoul: Korea, July 6-11, 2008.

Kocsis, L., Farkas, I., Mészáros, C., Teodorov, T., & Mellmann, J. (2009). Moisture content distributions comparison in semi-technical and industrial mixed-flow dryers. In *Proceedings of the 4th Nordic drying Conference*. Iceland: Reykjavik. June 17-19, 2009.

Kunibert, M. (1983). *Transport, Umschlag, Lagerung in der Landwirtschaft*. Berlin: VEB Verlag Technik.

Liu, Q. (1993). *Study on the drying mechanism, simulation and test of mixed flow grain dryer*. Ph.D. Thesis, Beijing Agricultural Engineering University.

Liu, Q., Montross, M. D., & Bakker-Arkema, F. W. (1997). Stochastic modelling of grain drying: Part 1. Experimental Investigation. *Journal of Agricultural Engineering Research, 66*, 267–273.

Liu, H., Zhang, J., Tang, X., & Lu, Y. (2003). Fuzzy control of mixed-flow grain dryer. *Drying Technology, 21*, 807–819.

Liu, X., Chen, X., Wu, W., & Zhang, Y. (2006). Process control based on principal component analysis for maize drying. *Food Control, 17*, 894–899.

Luding, S. (2008). Cohesive, frictional powders: contact models for tension. *Granular Matter, 10*, 235–246.

Maier, D. E., & Bakker-Arkema, F. W. (2002). Grain drying Systems. In *Proceedings of the 2002 Facility design Conference of the grain elevator & processing Society* (pp. 1–53), St. Charles, Illinois, U.S. A., July 28-31.

Markauskas, D., Kačianauskas, R., Džiugys, A., & Navakas, R. (2010). Investigation of adequacy of multi-sphere approximation of elliptical particles for DEM simulations. *Granular Matter, 12*, 107–123.

McFarlane, N. J. B., & Bruce, D. M. (1991). Control of mixed-flow grain driers: Development of a Feedback-plus-Feedforward Algorithm. *Journal of Agricultural Engineering Research, 49*, 243–258.

Mellmann, J., Richter, I.-G., & Maltry, W. (2007). Experiments on hot-air drying of wheat in a semi-technical mixed-flow dryer. *Drying Technology, 25*, 1287–1295.

Mellmann, J., Iroba, K. L., Möller, B., Metzger, T., & Tsotsas, E. (2010). Moisture content and residence time distributions in mixed-flow grain dryers. In *Proceedings of the 17th International Drying Symposium (IDS2010), Magdeburg, Germany, October 3-6, 2010*. pp. 1995–202002.

Mellmann, J., & Teodorov, T. (2011). Solids transport in mixed-flow dryers. *Powder Technology, 205*, 117–125.

Mohsenin, N. N. (1970). *Physical properties of plants and Animal Materials, Vol 1*. New-York: Gordon and Breach Science Publishers Inc.

Mühlbauer, W. (2009). *Handbuch der Getreidetrocknung*. Clenze (Germany): AgriMedia Verlag.

Nellist, M. E., & Bruce, D. M. (1995). Heated-Air grain drying. In D. S. Jayas, N. D. G. White, & W. E. Muir (Eds.), *Stored-Grain Ecosystems* (pp. 609–659). New York: Marcel Dekker Inc, (Chapter No. 16.

Pabis, S., Jayas, D. S., & Cenkowski, S. (1998). *Grain drying*. New York: Wiley & Sons.

Sokhansanj, S., & Lang, W. (1996). Prediction of kernel and bulk volume of wheat and Canola during Adsorption and Desorption. *Journal of Agricultural Engineering Research, 63*, 129–136.

Sun, L., Arnaud, G., & Fohr, J.-P. (1992). Heat and moisture transfer between ducts in an industrial cereal drier. In A. S. Mujumdar (Ed.), *Drying '92, Proceedings of the 8th International drying Symposium (IDS'92), Montreal, Canada, August 2-5, 1992* (pp. 1399–1407). Amsterdam: Elsevier Science Publishers B.V.